3D Printing of Auxetic Shape-Memory Metamaterial towards Designable Buckling

Zhenghong Li[1], Yuheng Liu[1], Yafei Wang[1], Haibao Lu[1,2]*, Ming Lei[3**] and Yong Qing Fu[4]

[1]Science and Technology on Advanced Composites in Special Environments Laboratory, Harbin Institute of Technology, Harbin 150080, China
[2]Key Laboratory of Micro-Systems and Micro-Structures Manufacturing of Ministry of Education, Harbin Institute of Technology, Harbin, 150080, China

[3]School of Astronautics, Northwestern Polytechnical University, Xi'an, 710072, PR China

[4]Faculty of Engineering and Environment, University of Northumbria, Newcastle upon Tyne, NE1 8ST, UK

* Corresponding author. Email address: luhb@hit.edu.cn

** Corresponding author. Email address: leiming@nwpu.edu.cn

As one of the most popular 3D printed metamaterials, the auxetic structure with its tunable Poisson's ratio has attracted huge amount of attention recently. In this study, we designed an auxetic shape-memory metamaterial, which showed designable buckling responses by using the thermomechanically coupled in-plane instability. The influence of viscoelasticity on in-plane moduli and Poisson's ratios of shape memory auxetic metamaterial was experimentally investigated. Based on the generalized Maxwell model and finite-element method, the buckling behaviors and their main influence factors were studied. The analytical results and experimental ones showed a good agreement. Thermomechanical properties of the printed metamaterials govern the temperature and strain-rate dependent buckling, and a controllable transition from

the negative to positive Poisson's ratio in the metamaterials can be achieved. Based on the shape memory effect, the buckled state and the Poisson's ratio of the metamaterials can be tuned by programmed thermomechanical processes. This study provides a simple and efficient way to generate morphing structures using the designable buckling effect.

Keywords: Metamaterial; 3D printing; shape memory polymer; buckling

1. Introduction

The volume change of materials and structures under external loads is mainly characterized by the Poisson's ratio. For a structure with a positive Poisson's ratio under uniaxial compression, the structure usually shrinks, and the length of its transvers axis (perpendicular to the compression direction) expands slightly with a Poisson's ratio,  . For the solid with  , the volume would remain a constant during compression, and the solid is usually termed as incompressible [Treloar. L. 1975]. Whereas for a material with a negative Poisson's ratio, e.g., 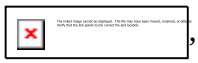 , the uniaxial compression would lead to an expansion of the material, and the tensile deformation would lead to a shrinking of the material. For example, a honeycomb structure showed a zero Poisson's ratio under a unidirectional deformation, and no deformation occurs in the vertical direction under in-plane stretching or compression [Grima *et al.*, 2010]. This abnormal stretch-induced shrinkage phenomenon is an interesting property that natural materials don't have. Therefore, the structures with negative Poisson's ratios are usually termed as auxetic mechanical metamaterials,

which have possessed many excellent properties, such as high expansibility, negative thermal expansion, high impact resistance, and facile programmability [Qu *et al.*, 2020; Babaee *et al.*, 2013; Bertoldi *et al.*, 2010; Lakes, 1987; Preston *et al.*, 2019; Qu *et al.*, 2017; Treml *et al.*, 2018; Wang *et al.*, 2016]. These properties enable their great potentials in the practical applications of packaging engineering, vehicle and aerospace fields [Coulais *et al.*, 2016; Ding *et al.*, 2017; Maconachie *et al.*, 2019].

The abnormal auxetic properties depend on the structural design of the metamaterial, and therefore it has attracted great attention to significantly improve the structure's designs. To achieve the auxetic design, Boyce *et al.* prepared a periodic porous elastomer, which showed a loading instability and a compression-induced shrinkage behavior after reaching the critical loading point [Boyce *et al.*,2007]. Bertoldi *et al.* designed a two-dimensional elastic plate with open holes arranged in a lattice pattern, thus enabling the transformation of pore structures between the ellipse structure and the expanded one in the uniaxial loading [Bertoldi *et al.*,2010]. However, most of these previous studies are focused on the quasi-static responses of the mechanical metamaterials, and acoustic wave and wave conduction characteristics were also studied for their dynamic behaviors [Babaee *et al.*, 2016; Celli *et al.*, 2018; Celli *et al.*, 2019; Cummer *et al.*, 2016; Frenzel *et al.*, 2019; Kadic *et al.*, 2019].

Polylactic acid (PLA) material is selected due to its viscoelastic nature and shape memory effect. Its biodegradable aliphatic polyesters are well suitable for both disposable applications and shape memory material with a well-defined glass-

transition temperature. These will be crucial for achieving good temperature responses in our designed structure. This article is focused on the studies of structure changes near the glass transition temperature. There are other types of materials which could be used for the study [Sun *et al.*, 2017, Zhou *et al.*, 2015]. In addition to the structure designs, the dynamic mechanical behaviors of different viscoelastic materials at different temperatures are quite different. By studying the influences of loading temperatures and strain rates on the constituent materials [Bauwens, 1973; Siviour and Jordan, 2016], and furthermore on the mechanical instability of the thermomechanical metamaterials, we can fully understand their working principles and the evolution mechanisms of Poisson's ratios [Jordan *et al.*, 2008; Siviour *et al.*, 2005]. To reveal the thermomechanical properties of the constituent materials, Jordan *et al.* [Jordan *et al.*, 2008] studied the dynamic yielding behavior of polyvinyl chloride (PVC) mechanical metamaterial at the strain rates of 10^{-3}~10^{4}/s. They found that the yield strength of the PVC was significantly improved with an increase in the strain rate. Janbaz *et al.* combined hyperplastic silicone rubber with viscoelastic polylactic acid (PLA) to design a double beam structure, of which both the positive and negative Poisson ratios were achieved in response to various strain rates [Janbaz *et al.*, 2020].

The dynamic behaviors of these metamaterials are strongly dependent on the pre-deformed processes and are seriously limited by the intrinsic properties of the material matrixes, thus resulting in the auxetic performances non-designable and inconsistent [Hajighasemi *et al.*, 2020; Liu *et al.*, 2020]. Janbaz and other workers studied the

dynamic mechanical behavior of a variety of materials [Dykstra *et al.*, 2019, Janbaz *et al.*, 2020]. However, research on the dynamic auxetic responses has not received extensive attention.

Shape memory polymers (SMPs), whose temporary shapes can be fixed, and then recovered to their permanent shapes in response to external stimuli, have been extensively studied. They are also used to achieve the continuously dynamic auxetic responses [Charlesby, 1960; Charlesby *et al.*, 1987; Essassi *et al.*, 2019; Essassi *et al.*, 2020; Odian and Bernstein, 1964]. Meanwhile, 3D printing technology provides the chances for the shape memory effect (SME) of the SMP matrix with a time evolution, resulting in the so-called 4D printing structure with a capability of in-plane pattern switching due to the SME [Huang *et al.*, 2020; Lei *et al.*, 2019].

The objective of this study is to develop a tailorable auxetic metamaterial by combining SME of polylactic acid (PLA) and additive manufacture as shown in Fig. 1. The shape-memory metamaterial undergoes a tunable buckling response by means of thermomechanical coupling and in-plane elastic instability. Simulations were firstly performed in order to obtain the information of the Poisson's ratios and transverse strains of the unit cell, as shown in Figs. 1(A) and 1(B). These analytical simulations were then verified using the experimental results and *in-situ* observation at different temperatures and strain ratios. The dependences of in-plane moduli and Poisson's ratios of auxetic PLA shape-memory metamaterials on viscoelasticity were then identified to be the main contribution to the thermomechanical coupled instability.

Thermomechanical buckling transition behavior of the auxetic metamaterials, from negative to positive Poisson's ratio, was further investigated as a function of geometrical morphology, temperature and strain rate. Finally, the tunable buckling transitions were achieved by the SMEs in the PLA SMP, resulting from the temperature-dependent shape programming and memory behaviors, as shown in Fig. 1(C).

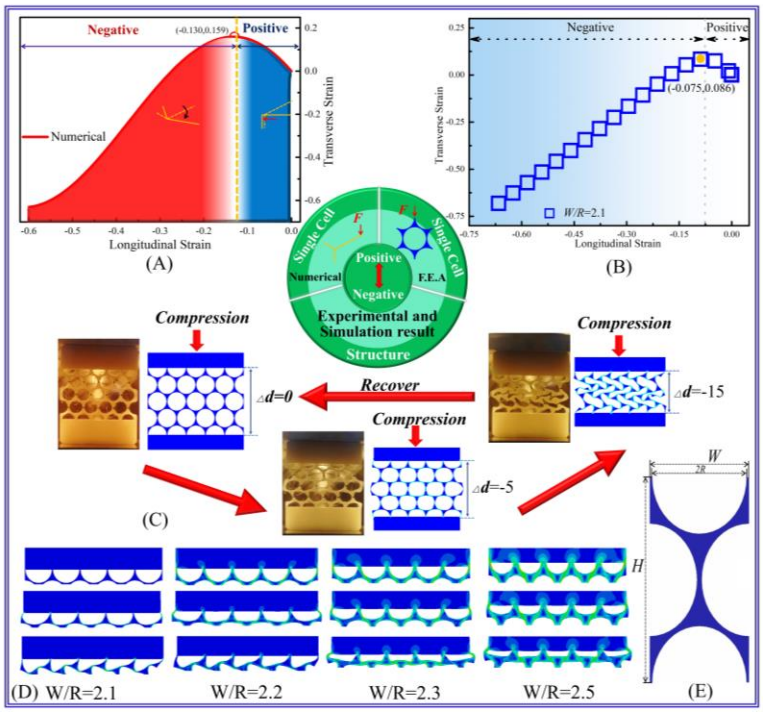

Fig. 1. The diagrammatic sketch of the auxetic shape-memory metamaterials. (A) Simulation results of the transition behavior of cell structure from the positive to negative Poisson's ratio. (B) Finite-element analysis (FEA) of the transverse strain as a function of longitudinal strain for the cell structure with the ratio of the thickness (W) to the radius (R), *i.e.*, W/R =2.1. (C) Experimental and simulation results of the shape programming and recovering behavior of 3D printing SMP lattice structure.

2. Design and Experiments

2.1 Designs

The unit cell was designed using the SolidWorks (3DS Dassault systems, France), in which a 2D square lattice configuration of the auxetic shape-memory metamaterial was assembled, as shown in Fig. 1(C). In this case, the free boundary has little effect on the mechanical behavior of the whole structure [Lei *et al.*, 2018]. For the auxetic shape-memory metamaterial, both the geometry and in-plane modulus were determined using the porosity parameter. Whereas the porosity was tailored by the ratio of thickness (W) to radius (R) in the unit cell as shown in Fig. 1(E), *i.e.*, W/R=2.1, 2.2, 2.3 and 2.5. The thicknesses of these lattice structures were 12mm. In order to prevent out-of-plane buckling of the structure during compression, its top and bottom were fixed. Stress concentration occurred at the intersection of the fix ends and the structure (as revealed in Fig. 1D).

2.2 Materials and Experiments

All the testing samples were fabricated by using a 3D fused filament fabrication (FFF) printer (Hyrel Engine, Hyrel International Inc., Atlanta, GA, USA). PLA filament (Natural PRO Series PLA Filament, Matter Hackers Inc., CA, USA) was used as the polymeric material. The glass transition temperature of PLA is ~70^{o}C, and the Young's modulus at room temperature (25^{o}C) is ~2.4 GPa. The printing temperature was 210^{o}C and the printing-bed temperature was 60^{o}C. The moving speed of the print tip was set as 20 mm/s.

Uniaxial tensile tests were carried out at 25^{o}C to characterize the mechanical properties of PLA based shape-memory metamaterials. The strain-controlled compressive loads were applied on the metamaterial using a universal material testing machine (Zwick-010, Zwick Roell Group, Germany) at a constant speed of 0.1 mm/s. Dynamic mechanical analysis (DMA, DMA861E, Mettler Loledo, Switzerland) was employed to investigate the thermomechanical responses of the PLA shape-memory metamaterials, in a temperature range from -30^{o}C to 110^{o}C, with a heating rate of 2^{o}C/min. The temperature scanning was performed in a uniaxial tensile mode. The strain was oscillated at a frequency of 1 Hz with a peak amplitude of 0.1%, and a small preloading strain of 0.001 N was applied during the test.

2.3 FE analysis

To analyze the deformation behavior of the designed metamaterials, the commercial software ABAQUS (3DS Dassault systems) was used for FEA. Thermodynamic behaviors of the PLA metamaterials were well described using the viscoelastic general Maxwell model [Ge *et al.*, 2014; Lei *et al.*, 2017; Wang *et al.*, 2013] as a user-coded subroutine in ABAQUS software, and the loading conditions in the FEA process was the same as those of the experiment conditions. Meanwhile, to improve the efficiency of the computational process, we designed a representative element and then applied the periodic boundary conditions to these elements. Finally, a complete geometric model was built in order to calculate the deformation of the whole structure.

The same boundary conditions as those of the experimental ones were applied to carry out the FEA.

3. Results and Discussion

3.1 Transition behavior of Poisson's ratio for the unit cell

To investigate the buckling transition of shape-memory metamaterial from the positive to negative Poisson's ratio, the mechanical behaviors of the unit cells, which have various ratios of thickness (W) to radius (R), e.g., W/R=2.1, 2.2, 2.3 and 2.5, have been firstly studied by the FEA. The results are shown in Fig. 2. As designed, the stiffness is significantly influenced by the W/R of the metamaterials. The modulus is gradually increased with an increase in the W/R. When the radius of hole, R, is small, the unit cell undergoes bending, and the second moment of the section area determines the stiffness of the structure. On the other hand, when R is large, the unit cell undergoes stretching, thus resulting in the stiffness determined by the section area.

Under a compression loading along the y axis, the unit cell gradually becomes twisted. Initially, the transverse strain along the x axis is gradually increased from 0 to 8.6% with a decrease in the longitudinal strain from 0 to -7.5%, for the unit cell with a W/R of 2.1. The longitudinal Poisson's ratio is -1.15. Furthermore, the unit cell becomes showing an auxetic behavior and achieves a negative Poisson's ratio with a further change of longitudinal strain from -7.5% to -60%. The similar buckling transitions are also revealed by the unit cells with W/R of 2.2, 2.3 and 2.5, whereas the unit cells undergo transitions from positive to negative Poisson's ratios with the

longitudinal strains of -4.2%, -8.3% and -7.7%, respectively. The longitudinal negative Poisson's ratios are -1.31, -0.59 and -0.60, respectively. These analytical results demonstrate that the configuration structure, which determines the stiffness by means of porosity and *W*/*R*, has a significant effect on the buckling behavior of the unit cell.

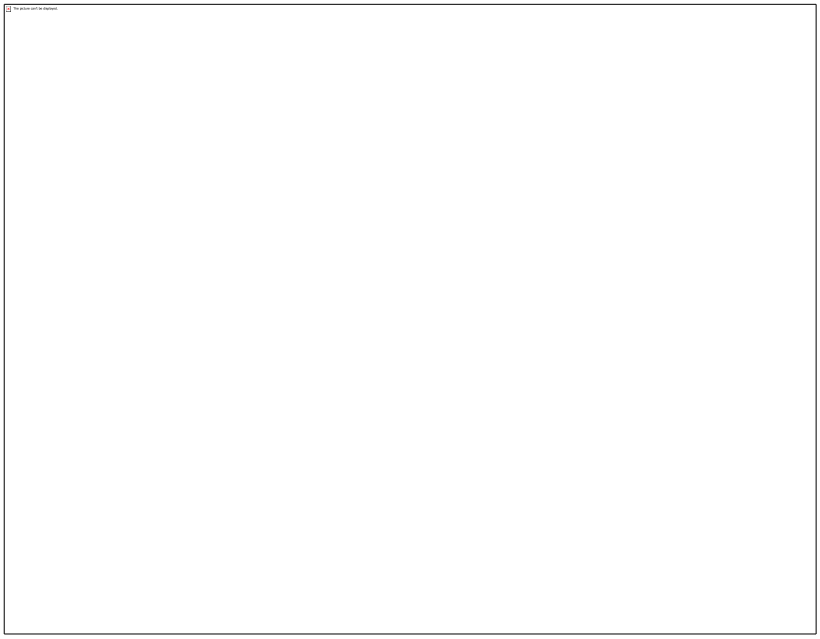

Fig. 2. Designs and auxetic transition behaviors of the unit cells with different *W*/*R* ratios.

3.2 Programming by shape memory effects

The printed 2D-lattice structure can be programmed into different geometries due to the SME of PLA SMP. A typical shape memory cycle is incorporated of two processes, *i.e.*, a shape programming process and a shape recovering process as shown in Fig. 3. To program the printed lattice structure with a length of 84.67 mm to have the SME (as shown in Fig. 3(AI)), it was initially heated at 80^{o}C for 10 min, and then

compressed to the programmed deformation of 69.11 mm, followed by holding the applied strain for another 10 min. It was found that the deformed shape was fixed after cooling down to 25°C and removing the mechanical loading, as shown in Fig. 3(AII). To regain the initial shape, the lattice structure was reheated up to 80°C, and experimental result revealed that the deformed shape of the lattice structure was then triggered and recovered to its original shape (83.86 mm), as shown in Fig. 3(AIII). Meanwhile, the shape recovery process of the metamaterials was demonstrated by pre-deformed at room temperature and then heated up to 80°C, as shown in Fig. 3(B). The sample took ~15 s to complete the whole shape recovery at 80°C.

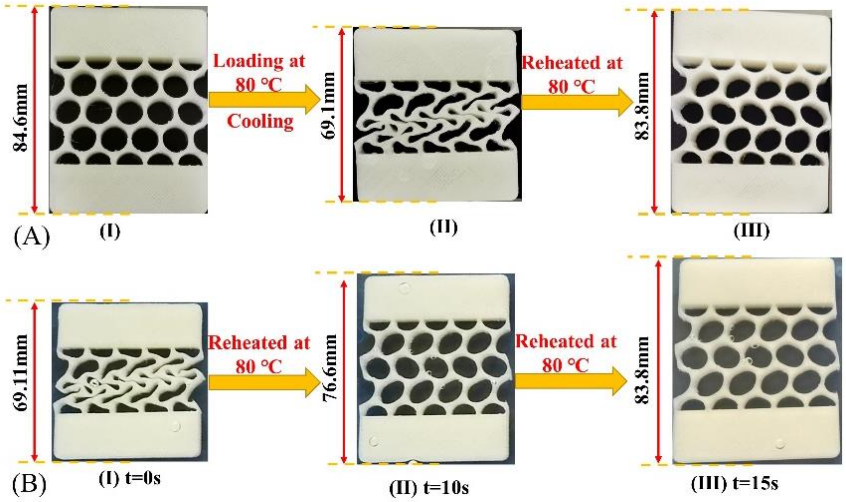

Fig. 3. The shape program and recovery of the printed PLA lattice structure. (A) For the shape program process. (B) For the shape recovery process.

To evaluate the mechanical properties of the PLA lattice structures with different *W*/*R* ratios, the tensile experiments were carried out and the stress-stain curves were recorded. The results are shown in Fig. 4. Figure 4(A) shows that the PLA lattice structures present an approximately linear elastic behavior at 25°C [Yarali and Taheri,

2020]. The breaking strains are varied from 2.0 to 3.0. On the other hand, the lattice structures reveal the non-linear viscos-elasticity at 80°C, which is above the glass transition temperature of PLA (~70°C). The yield stresses are presented in Fig. 4(B), and the longitudinal strains are significantly increased. Therefore, the viscoelastic behaviors of the PLA lattice structures have been achieved.

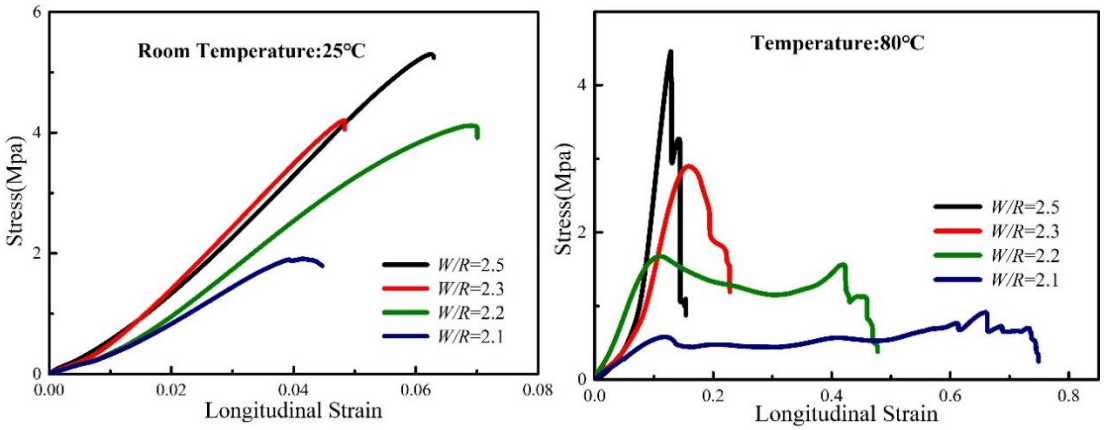

Fig. 4. The experimental stress-strain curves in tensile tests for the PLA lattice structures with *W*/*R* ratios of 2.1, 2.2, 2.3 and 2.5. (A) at 25°C; (B) at 80°C.

3.3 Design of temperature-dependent bulking transition

A reliable and predictable transition of the bucking could provide a good opportunity to design the geometrical and morphology-dependent mechanical metamaterials. Again, we still considered four PLA metamaterials with the *W*/*R* ratios of 2.1, 2.2, 2.3 and 2.5. The temperature-dependent transitions between the positive and negative Poisson's ratios were explored for the design of soft mechanisms.

To investigate temperature-dependent transitions from a positive to a negative value of the Poisson's ratio, five temperatures of 60°C, 65°C, 70°C, 75°C and 80°C

were applied on the PLA lattice structures for simulations. The afore-mentioned general Maxwell model was used to investigate the temperature-dependent transition behaviors. The changes of the Poisson's ratios were recorded as a function longitudinal strain, and the results are shown in Fig. 5. As revealed from Figure 5(A), the Poisson's ratios are positive with a decrease of the longitudinal strain from -14.5% for the lattice structure with W/R=2.1, at the temperature of 60^{o}C. The transition behavior is found to change at different longitudinal strains of -14.5%, -16.5%, -19.0%, -19.0% and -17.3%, with an increase of temperature from 60^{o}C, 65^{o}C, 70^{o}C, 75^{o}C to 80^{o}C. In Fig. 5(B), for the lattice structure with W/R=2.2, the transition behavior is found to change at the different longitudinal strains of 28.6%, 23.6% and 20.0%, with an increase in temperature from 70^{o}C, 75^{o}C to 80^{o}C. In Fig. 5(C), for the lattice structure with W/R=2.3, the transition behavior is found at two different longitudinal strains of 26.0% and 30.8%, with an increase in temperature from 75^{o}C to 80^{o}C. Meanwhile, there is no transition behavior observed for the lattice structure with W/R=2.5, as shown in Fig. 5(D).

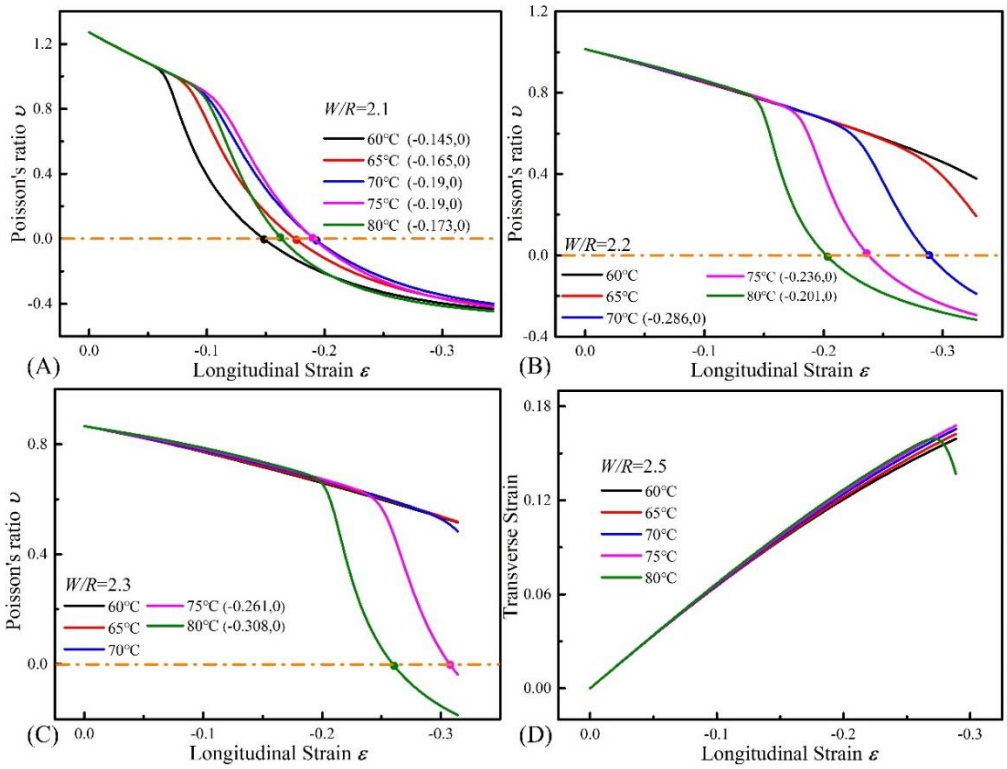

Fig. 5. Computationally predictions of the stress-strain relationship of the PLA metamaterials at the temperature of T =60°C, 65°C, 70°C, 75°C and 80°C (A) For lattice structure with *W*/*R*=2.1; (B) For lattice structure with *W*/*R*=2.2; (C) For lattice structure with *W*/*R*=2.3 and (D) For lattice structure with *W*/*R*=2.5.

For the PLA SMP, the stiffness is adaptive and tailorable based on the thermomechanical history, which determines the shape recovery behavior of PLA. The working mechanisms of temperature-dependent transition behavior from a positive to a negative Poisson's ratio and thermomechanical property are both originated from the viscoelastic behavior of the metamaterial, which will accelerate the chain mobility with an increase in temperature [Puskas *et al.*, 2006; Xu *et al.*, 2016]. Therefore, our computational predictions show that the mechanical transition

behavior of the PLA lattice structure is critically determined by the viscoelasticity and the glass transition behaviors of the metamaterial.

3.4 Design of strain rate-dependent bulking transition

To valid the effects of viscoelastic and thermomechanical property on the mechanical behavior, the strain-rate dependent yielding behavior of the PLA lattice structure has been studied using the FEA, and the results are shown in Fig. 6. Six compression strain rates of $0.002s^{-1}$, $0.011s^{-1}$, $0.022s^{-1}$, $0.109s^{-1}$, $0.219\ s^{-1}$ and $0.547\ s^{-1}$ were applied on the lattice structures, and the stress-strain curves have been recorded at temperatures of 60^oC, 70^oC and 80^oC. The obtained results are shown in Figs. 6(A), 6(B) and 6(C), respectively. As shown in Fig. 6(A), for the PLA lattice structure at 60^oC, the yield stress is gradually increased from 0.014 MPa, 0.020 MPa, 0.029 MPa to 0.041 MPa, with an increase in the compression strain rates from $0.002s^{-1}$, $0.011s^{-1}$, $0.022s^{-1}$ to $0.109s^{-1}$. Meanwhile, the yield stress is gradually increased from 0.010 MPa, 0.012 MPa, 0.014 MPa, 0.020 MPa, 0.025 MPa to 0.033 MPa with an increase in the compression strain rates from $0.002s^{-1}$, $0.011s^{-1}$, $0.022s^{-1}$, $0.109s^{-1}$, $0.219\ s^{-1}$ to $0.547\ s^{-1}$, as shown in Fig. 6(B). The yield stress is gradually increased from 0.008 MPa, 0.009 MPa, 0.010 MPa, 0.013 MPa, 0.015 MPa to 0.019 MPa with an increase in the compression speed from $0.002s^{-1}$, $0.011s^{-1}$, $0.022s^{-1}$, $0.109s^{-1}$, $0.219\ s^{-1}$ to $0.547\ s^{-1}$, as shown in Fig. 6(C). Results show that the strain rate plays an essential role to determine the mechanical behavior of the PLA lattice structure. At the same temperature, the yield stress is gradually increased with an increase in the strain rate.

While results also show that the yielding stress is gradually decreased from 0.014 MPa, 0.010 MPa to 0.008 MPa with an increase in the temperature from 60^{o}C, 70^{o}C to 80^{o}C, at the same compression strain rate of 0.002s^{-1}. These analytical results prove that the mechanical behavior is resulted from the viscoelastic and thermomechanical property of the PLA lattice structure.

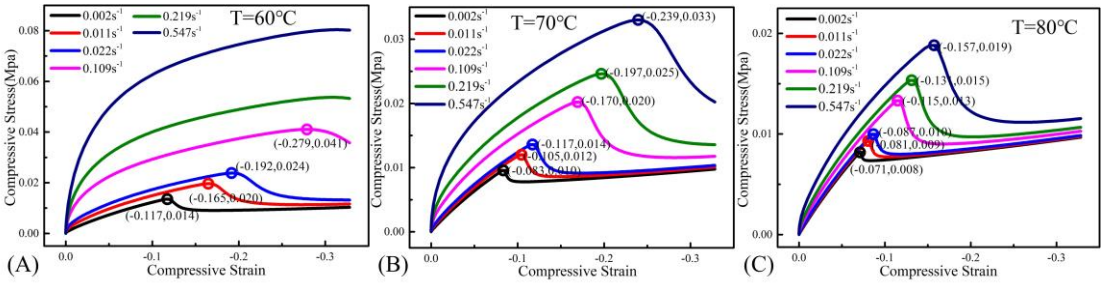

Fig. 6. Computationally predictions of the stress-strain relationship of the PLA metamaterials at the compression strain rates of 0.002s^{-1}, 0.011s^{-1}, 0.022s^{-1}, 0.109s^{-1}, 0.219 s^{-1} and 0.547 s^{-1}, where W/R=2.2. (A) At T=60^{o}C; (B) At T=70^{o}C; (C) At T=80^{o}C.

The evolution in the Poisson's ratio of FEA was also analyzed as a function of longitudinal strain as shown in Fig. 7. As revealed in Fig. 7(A), the transition from a positive to a negative Poisson's ratio becomes more significant at the longitudinal strains of -17.9%, -22.6% and -26.0%, with an increase in the compression speed from 0.002s^{-1}, 0.011s^{-1}, to 0.022s^{-1} for the lattice structure with W/R=2.2 at the temperature of 60^{o}C. In Fig. 7(B), the transition behaviors from a positive to a negative Poisson's ratios becomes more significant at the longitudinal strains of -16.7%, -17.3%, -17.9, -23.2%, -26.7% and -32.1% with an increase in the compression strain rates from 0.002s^{-1}, 0.011s^{-1}, 0.022s^{-1}, 0.109s^{-1}, 0.219 s^{-1} to 0.547

s^{-1} at the temperature of 70°C. Meanwhile, the transition behaviors from a positive to a negative Poisson's ratios becomes more significant at the longitudinal strains of -16.5%, -16.8%, -17.0, -17.8%, -19.0% and -22.3% with an increase in the compression strain rates from $0.002s^{-1}$, $0.011s^{-1}$, $0.022s^{-1}$, $0.109s^{-1}$, $0.219\ s^{-1}$ to $0.547\ s^{-1}$ at the temperature of 80°C, as shown in Fig. 7(C). These analytical results reveal that the transition behavior from a positive to a negative value of the Poisson's ratio was critically determined by the strain rate, when the PLA lattice structure was heated nearly to its glass transition temperature of 75°C. Therefore, the working principle behind these phenomena is originated from the thermomechanical viscoelastic properties of the PLA.

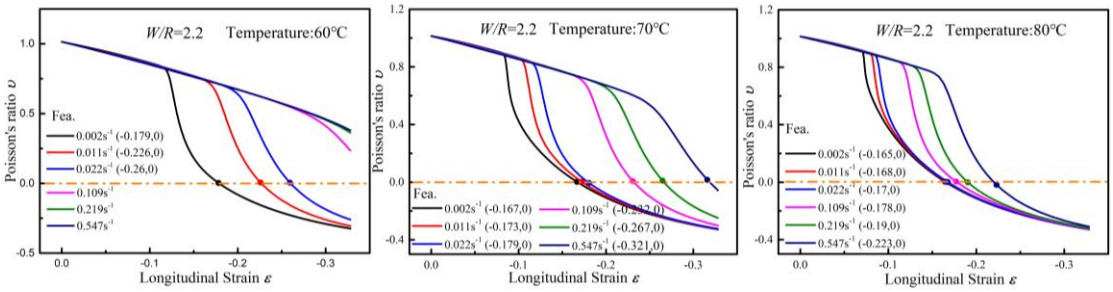

Fig. 7. Computationally predictions of the transition behavior from a positive to a negative value of the Poisson's ratio of PLA lattice structure at the compression strain rates of $0.002s^{-1}$, $0.011s^{-1}$, $0.022s^{-1}$, $0.109s^{-1}$, $0.219\ s^{-1}$ and $0.547\ s^{-1}$, where W/R=2.2. (A) At T=60°C; (B) At T=70°C; (C) At T=80°C.

Furthermore, Figure 8 presents a cloud chart of compressive speed and temperature dependent transition behaviors of PLA lattice structures from the positive to negative Poisson's ratios, where the W/R ratios are 2.1, 2.2, 2.3 and 2.5. Results

clearly show that there is a synergistic effect of compressive speed and temperature on the transition behavior of the PLA lattice structure. As discussed above, a high compressive speed always results in a high stiffness by significantly reducing the relaxation time of the structure, and further enables a conventional performance (e.g., positive Poisson's ratio) of the PLA lattice structure. On the other hand, a low stiffness is always achieved at a high temperature, resulting in an auxetic performance (e.g., negative Poisson's ratio) of the PLA lattice structure. Therefore, the PLA lattice structure presents a positive Poisson's ratio, resulted from the synergistic effects of high compressive speed and low temperature. While it reveals a negative Poisson's ratio, owing to the synergistic effects of low compressive speed and high temperature. The transition behavior from the positive to negative Poisson's ratio can be achieved using two strategies for the PLA lattice structure, i.e., depressing the compressive speed or increasing the temperature.

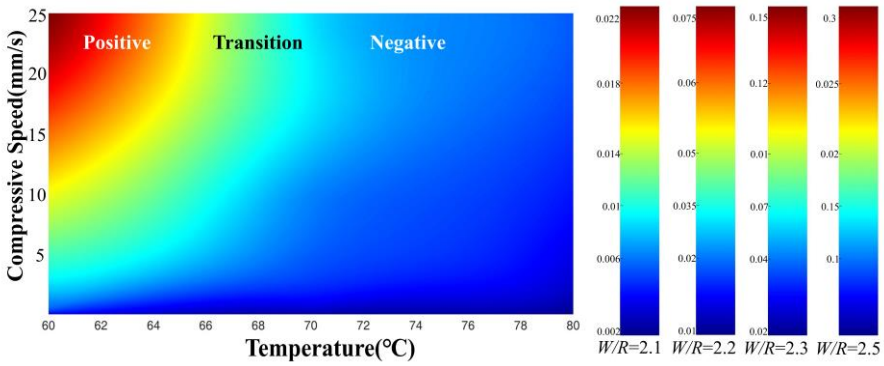

Fig. 8. The cloud chart of the transitions of PLA lattice structures from the positive to negative Poisson's ratios, as functions of temperature and strain rate.

3.5 A combined experimental and analytical study of PLA metamaterials

To experimentally evaluate the analytical results, four types of PLA lattice structures with the *W*/*R* ratios of 2.1, 2.2, 2.3 and 2.5 have been manufactured. To assess the validity of the proposed computational predictions, the analytical results of the computational models were used to show the viscoelastic and thermomechanical behaviors of the PLA lattice structures. Then the experimental results were also obtained and compared for the verification of the analytical ones. All the results are shown in Fig. 9. As revealed in Fig. 9(A) for the PLA lattice structure with *W*/*R*=2.1, it presents a distinct mechanical behavior at 60^{o}C in comparison with that at 70^{o}C and 80^{o}C, because the glass transition temperature of PLA is 70^{o}C. Therefore, the lattice structure reveals a glassy mechanical behavior at 60^{o}C, which is below the glass transition temperature of PLA. On the other hand, it reveals a rubbery mechanical behavior at 70^{o}C and 80^{o}C, which are equal to and above the glass transition temperature of PLA. The analytical results from the FEA models are in good agreements with the experimental data for the PLA lattice structure at 70^{o}C and 80^{o}C. However, there is a large divergence between analytical and experimental results at 60^{o}C. It can be attributed to the experimental error, which is mainly resulted from the defects in the lattice structure and it plays a significant effect on the stiffness in the glass state of PLA at a lower temperature. That is to say, the effect of defects in the lattice structure becomes more prominent when the PLA has a higher stiffness. While it becomes less significant when the PLA is heated above its glass transition temperature, due to the significantly reduced stiffness. Similar results have also been

found in Figs. 9(B), 9(C) and 9(D), for the PLA lattice structures with *W*/*R* of 2.2, 2.3 and 2.5, respectively.

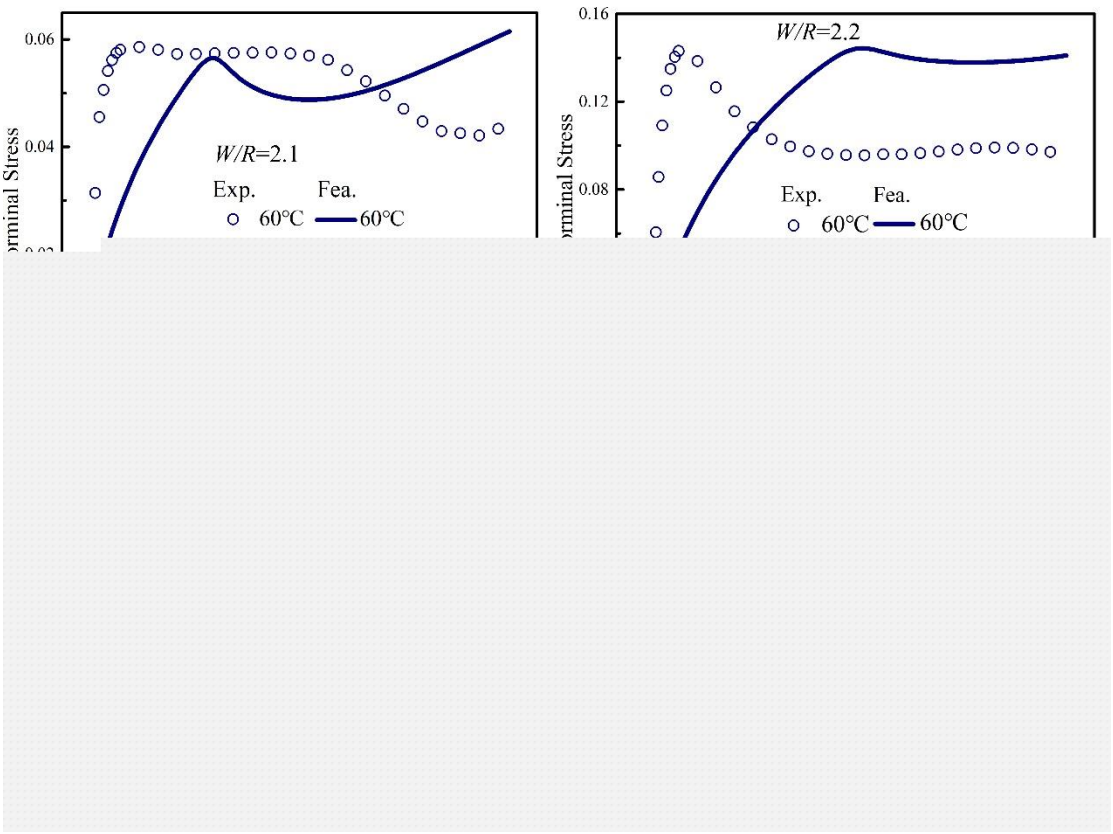

Fig. 9. Comparison between the stress-strain curves predicted by FE methods and the experimental observations of the PLA lattice structures at a variety of temperatures of 60°C, 70°C and 80°C. (A) For lattice structure with *W*/*R*=2.1; (B) For lattice structure with *W*/*R*=2.2; (C) For lattice structure with *W*/*R*=2.3 and (D) For lattice structure with *W*/*R*=2.5.

4. Conclusion

In this paper, we design a new periodically porous PLA SMP metamaterial inspired by the mechanoresponsive auxetic materials. Based on the FEA and experimental studies, tunable buckling responses by means of thermomechanical coupling and in-

plane elastic instability are achieved by the temperature and strain-rate dependent bulking of the PLA lattice structures. These analytical and experimental results verify that the transition of Poisson's ratio from the positive value to the negative one is mainly due to the SME and viscoelastic properties of PLA, which are used to achieve designable and tailorable buckling of lattice structure. The geometrical parameters and the loading conditions including temperatures, strain rates would strongly influence the instability transition. Finally, the analytical simulations had been verified using the experimental results. A good agreement between the computational results and experimental ones has been achieved. This paper is expected to provide the foundation for 3D printed mechanical metamaterials with programmable shape changes and tunable buckling transitions.

Acknowledgements

This work was financially supported by the National Natural Science Foundation of China (NSFC) under Grant No. 11725208.

References

Babaee, S., Shim, J., Weaver, J. C., Chen, E. R., Patel, N. and Bertoldi, K. [2013] "3D soft metamaterials with negative Poisson's ratio," *Advanced Materials* **25**(36), 5044–5049.

Babaee, S., Viard, N., Wang, P., Fang, N. X. and Bertoldi, K. [2016] "Harnessing deformation to switch on and off the propagation of sound," *Advanced Materials* **28**(8), 1631–1635.

Bauwens, C. [1973] "The compression yield behaviour of polymethyl methacrylate over a wide range of temperatures and strain-rates," *Journal of Materials Science* **8**(7), 968–97.

Bertoldi, K., Reis, P. M., Willshaw, S. and Mullin, T. [2010] "Negative Poisson's ratio behavior induced by an elastic instability," *Advanced Materials* **22**(3), 361-366.

Celli, P., Yousefzadeh, B., Daraio, C. and Gonella, S. [2018] "Exploring heterogeneity and disorder in tunable elastic metamaterials," *Journal of The Acoustical Society of America* **143**(3), 1917-1917.

Celli, P., Yousefzadeh, B., Daraio, C. and Gonella, S. [2019] "Bandgap widening by disorder in rainbow metamaterials," *Applied Physics Letters* **114**(9), 091903.

Charlesby, A. [1960] "In Atomic Radiation and Polymers," Vol. 1 (Ed:A. Charlesby), *Pergamon, Oxford*, UK 198.

Charlesby, A., Novakovic, L. and Gal, O. [1987] "Memory effect in irradiated polymers," *Radiation Physics and Chemistry* **30**(1), 67-68.

Coulais, C., Teomy, E., De, R. K., Shokef, Y. and Van, H. M. [2016] "Combinatorial design of textured mechanical matamaterials," *Nature* **7**(13), 529-535.

Cummer, S. A., Christensen, J. and Alù, A. [2016] "Controlling sound with acoustic metamaterials," *Nature Reviews Materials* **1**(3), 16001.

Ding, Z., Weeger, O., Qi, H. J. and Dunn, M. L. [2017] "4D rods: 3D structures via programmable 1D composite rods," *Materials & Design* **137**, 1-28.

Dykstra, D. M. J., Busink, J., Ennis, B., Coulais, C. [2019] "Viscoelastic snapping metamaterials," *Journal of Applied Mechanics* **86**(11), 111012.

Essassi, K., Rebiere, J. L., El Mahi, A., Ben Souf, M. A., Bouguecha, A. and Haddar, M. [2019] "Dynamic characterization of a bio-based sandwich with auxetic core: experimental and numerical study," *International Journal of Applied Mechanics* **11**(2), 1950016.

Essassi, K., Rebiere, J. L., El Mahi, A., Ben Souf, M. A., Bouguecha, A. and Haddar, M. [2020] "Investigation of the static behavior and failure mechanisms of a 3D printed bio-based sandwich with auxetic core," *International Journal of Applied Mechanics* **12**(5), 2050051.

Frenzel, T., Köpfler, J., Jung, E., Kadic, M. and Wegener, M. [2019] "Ultrasound experiments on acoustical activity in chiral mechanical metamaterials," *Nature Communications* **10**, 3384.

Ge, Q., Luo, X., Iversen, C. B., Nejad, H. B., Mather, P. T., Dunn, M. L. and Qi, H. J. [2014] "A finite deformation thermomechanical constitutive model for triple shape polymeric composites based on dual thermal transitions," *International Journal of Solids and Structures* **51**(15), 2777–2790.

Grima J. N., Oliveri L., Attard D., Ellul, B., Gatt, R., Cicala, G. and Recca, G. [2010] "Hexagonal Honeycombs with Zero Poisson's Ratios and Enhanced Stiffness," *Advanced Engineering Materials* **12**(9), 855–862.

Hajighasemi, M. R., Safarabadi, M., Sheidaei, A., Baghani, M. and Baniassadi, M. [2020] "A finite element framework for magneto-actuated large deformation and instability of slender magneto-active elastomers," *International Journal of Applied Mechanics* **12**(1), 2050013.

Huang, R., Zheng, S. J., Liu, Z. S. and Ng, T. Y. [2020] "Recent advances of the constitutive models of smart materials-hydrogels and shape memory polymers," *International Journal of Applied Mechanics* **12**(2), 2050014.

Janbaz, S., Narooei, K., Van, M. T. and Zadpoor, A. A. [2020] "Strain rate–dependent mechanical metamaterials," *Science advances* **6**(25), eaba0616.

Jordan, J. L., Foley, J. R. and Siviour, C. R. [2008] "Strain rate-dependant mechanical properties of OFHC copper," *Mechanics of Time-Dependent Materials* **48**(20), 7134–7141.

Kadic, M., Milton, G. W., Hecke, M. V. and Wegener, M. [2019] "3D metamaterials," *Nature Reviews Physics* **1**, 198–210.

Lakes, R. [1987] "Foam structures with a negative Poisson's ratio," *Science* **235**(4792), 1038–1040.

Lei, M., Yu, K., Lu, H. and Qi, H. J. [2017] "Influence of structural relaxation on thermomechanical and shape memory performances of amorphous polymers," *Polymer* **109**, 216–228.

Lei, M., Hamel, C. M., Yuan, C., Lu, H. B. and Qi, H. J. [2018] "3D printed two-dimensional periodic structures with tailored in-plane dynamic responses and fracture behaviors," *Composite Science & Technology* **159**, 189−198.

Lei, M., Hong, W., Zhao, Z., Hamel, C., Chen, M., Lu, H. B. and Qi, H. J. [2019] "3D printing of auxetic metamaterials with digitally reprogrammable shape," *ACS Applied Materials & Interfaces* **11**(25), 22768-22776.

Liu, Y., Chen, S. E., Tant, X. B. and Cao, C. Y. [2020] "A finite element framework for magneto-actuated large deformation and instability of slender magneto-active elastomers," *International Journal of Applied Mechanics* **12**(1), 2050013.

Maconachie, T., Leary, M., Lozanovski, B., Zhang, X. and Brandt, M. [2019] "Slm lattice structures: properties, performance, applications and challenges," *Materials & Design* **183**, 108137.

Mullin, T., Deschanel, S., Bertoldi, K. and Boyce, M. C. [2007] "Pattern transformation triggered by deformation," *Physical Review Letters* **99**(8), 084301.

Odian, G. and Bernstein, B. S. [1964] "Memory effects in irradiated polyethylene," *Journal of Applied Polymer Science* **8**(4), 1853-1867.

Preston, D. J., Rothermund, P., Jiang, H. J., Nemitz, M. P., Rawson, J., Suo, Z. and Whitesides, G. M. [2019] "Digital logic for soft devices," *Proceedings of The National Academy of Sciences of The United States of America* **116**(16), 7750–7759.

Puskas, J. E., Chen, Y., Kulbaba, K., Kaszas, G. and Soleymannezhad, A. [2006] "Effect of the molecular weight and architecture on the size and glass transition of arborescent polyisobutylenes," *Journal of Polymer Science Part A-Polymer Chemistry* **44**(5), 1770–1776.

Qu, J., Kadic, M., Naber, A. and Wegener, M. [2017] "Micro-structured two-component 3D metamaterials with negative thermal-expansion coefficient from positive constituents," *Scientific Reports* **7**, 40643.

Siviour, C. R., Walley, S. M., Proud, W. G. and Field, J. E. [2005] "The high strain rate compressive behaviour of polycarbonate and polyvinylidene difluoride," *Polymer* **46**(26), 12546-12555.

Siviour, C. R. and Jordan, J. L. [2016] "High strain rate mechanics of polymers: a review," *Journal of the Mechanical Behavior of Biomedical Materials* **2**(1), 15–32.

Sun. L., Huang. W. M., Wang. T. X., Chen. H. M., Renata. C., He, L. W., Lv. P., Wang, C. C. [2017] "An overview of elastic polymeric shape memory materials for comfort fitting," *Materials and Design* **136**, 238-248.

Treloar, L. R. G. 1975 The physics of rubber elasticity New York: Oxford University.

Treml, B., Gillman, A., Buskohl, P. and Vaia, R. [2018] "Origami mechanologic," *Proceedings of The National Academy of Sciences of The United States of America* **115**(27), 6916–6921.

Wang, A., Li, G. and Meng, H. [2013] "Strain rate effect on the thermomechanical behavior of a thermoset shape memory polymer," *Smart Materials and Structures* **22**(8), 085033.

Wang, Q., Jackson, J. A., Ge, Q., Hopkins, J. B., Spadaccini, C. M. and Fang, N. X. [2016] "Lightweight mechanical metamaterials with tunable negative thermal expansion," *Physics Review Letters* **117**(17), 175901.

Xu, W. S., Douglas, J. F. and Freed, K. F. [2016] "Influence of cohesive energy on relaxation in a model glass-forming polymer melt," *Macromolecules* **49**(21), 8355–8370.

Zhong, D., Xiang, Y. H., Liu, J. J., Chen, Z., Zhou, H. F., Yu, H. H., Qu, S. X. and Yang, W. [2020] "A constitutive model for multi network elastomers pre-stretched by swelling," *Extreme Mechanics Letters* **40**, 100926.

Zhou. Y., Huang. W. M., Kang. S. F., Wu. X. L., Lu. H. B., Fu. J., Cui. H.P. [2015] "From 3D to 4D printing: approaches and typical applications," *Journal of Mechanical Science and Technology* **29**(10), 4281-4288.